

Transverse thermoelectric transport in a model of many competing order parameters

Gideon Wachtel and Dror Orgad

Racah Institute of Physics, The Hebrew University, Jerusalem 91904, Israel

(Dated: October 31, 2018)

Coexisting fluctuations towards various ordered states are ubiquitous in strongly correlated electronic systems. In particular, measurements of underdoped cuprate high-temperature superconductors reveal evidence for short range charge order in parallel to large superconducting fluctuations. Here we use a non-linear sigma model to describe a system with N competing orders, and calculate its transverse thermoelectric transport coefficient in the analytically tractable limit of large N . Our results, which determine the contribution of order parameter fluctuations to the Nernst signal, are appropriate for high temperatures in the case of finite N . They are similar to previously obtained results within a model of Gaussian superconducting fluctuations.

I. INTRODUCTION

The nature of the pseudogap regime of underdoped cuprate high-temperature superconductors is still under debate¹. Studies have conjectured² that superconducting (SC) fluctuations survive over a large range of temperatures above the transition temperature, T_c . The large Nernst signal³⁻⁶ measured above T_c has been used to justify this viewpoint, since the Nernst effect is generally small in non-magnetic metals, and is large in the vortex state of superconductors. While the Nernst effect in the vortex state has been well understood for many years⁷, Ussishkin *et al.*⁸ were the first to theoretically consider it in a model of fluctuating superconductivity above T_c . They calculated the transverse thermoelectric transport coefficient within the Gaussian limit of a time-dependent Ginzburg-Landau (TDGL) model. For two-dimensional systems, which constitute the focus of our interest, this model can describe superconducting fluctuations far above the Berezinskii-Kosterlitz-Thouless transition temperature, T_{BKT} . Their results agree with Nernst measurements in amorphous $\text{Nb}_{0.15}\text{Si}_{0.85}$ films^{9,10} and in overdoped, but not underdoped cuprates⁸, where phase fluctuations¹¹, specifically thermally excited vortices^{12,13}, may be required to explain the Nernst effect closer to T_{BKT} .

Over the last few years, X-ray scattering from the pseudogap state of underdoped cuprates¹⁴⁻²⁰ has revealed charge density wave (CDW) order whose strength diminishes upon cooling below T_c , thereby indicating a competition between this order and superconductivity. Hence, it is desirable to reconsider the Nernst effect within a theory which incorporates the observed competition. A CDW order can affect the Nernst signal in a couple of ways. One route²¹ is via the CDW's effect on quasiparticles, which can in turn change the measured Nernst signal. The second route, which we consider here, is its competition with SC fluctuations. Above T_{BKT} the CDW fluctuations are important in determining the properties of thermally excited SC vortices²² and consequently the size of the Nernst signal. At even higher temperatures, where thermally excited vortices begin to overlap, Ussishkin *et al.*'s results for the Gaussian TDGL are ex-

pected to hold, provided one properly accounts for the effect of the competing CDW.

Recently, Hayward *et al.*²³ formulated the competition between the SC and CDW order parameters using a phenomenological non-linear sigma model (NLSM). By running Monte-Carlo simulations of their model, they were able to reproduce the temperature dependence of the CDW structure factor as observed in the X-ray experiments. In addition, they treated the model analytically in the case of a large number, N , of order parameter components. Using a saddle-point approximation and including $1/N$ corrections they were able to reproduce the numerical results for the CDW structure factor and to calculate the diamagnetic susceptibility at high temperatures. Their result for the latter agrees with the expected behavior from Gaussian SC fluctuations.

The transverse thermoelectric transport coefficient, α_{xy} , is defined as the ratio between an applied temperature gradient, $-\partial_y T$, and the resulting transverse electric current, J_x , *i.e.*, $J_x = \alpha_{xy}(-\partial_y T)$. For systems with particle-hole symmetry or when SC fluctuations dominate, the experimentally measured Nernst signal is given by⁶ $e_N = \rho \alpha_{xy}$, where ρ is the longitudinal resistivity. The purpose of this paper is to calculate α_{xy} at high temperatures using the $N \rightarrow \infty$ limit of Hayward *et al.*'s model. For simplicity we consider the fully $O(N)$ symmetric case, but the results can be generalized to a more experimentally relevant model, where the symmetry is not exact. Unlike the magnetization, which is calculated in equilibrium, the Nernst effect is a transport phenomenon which must be addressed within a dynamical model. Here we assume that the SC and CDW fields obey a (Model A) generalized Langevin equation²⁴. Using a path integral approach²⁵ to the Martin-Siggia-Rose formalism²⁶, we calculate diagrammatically the system's response to weak perturbations. As expected, we find that α_{xy} agrees with Ussishkin's results for the Gaussian TDGL model. We chose to include here the complete and detailed calculation, as we believe it has pedagogical value of its own.

The paper is outlined as follows. The model, its Langevin dynamics and the path integral approach that we use are presented in section II. Section III describes the saddle-point approximation which is em-

ployed throughout the paper. In section IV we summarize various diagrams which are then used to calculate the diamagnetic susceptibility, in section V, and α_{xy} in section VI. We conclude with a discussion in section VII. Some details of the calculation are relegated to the appendices.

II. MODEL AND DYNAMICS

We start by considering an $O(N)$ symmetric Ginzburg-Landau model of N real order parameters, n_α , $\alpha = 1 \dots N$, competing with each other:

$$F = \int d^2r \left\{ \frac{\rho_s}{2} \sum_\alpha (\nabla n_\alpha)^2 + \frac{u}{4N} \left(\sum_\alpha n_\alpha^2 - N \right)^2 \right\}. \quad (1)$$

The non-linear sigma model (NLSM), with the constraint,

$$\sum_\alpha n_\alpha^2 = N, \quad (2)$$

is obtained²⁷ from (1) by taking the limit $u \rightarrow \infty$. In order to study transport phenomena we need to introduce dynamics into the model. A simple approach, which we follow here, is to assume that the order parameters n_α obey stochastic dynamics, without any conservation constraints (model A of Ref. 24). Thus, the time dependence of the fields n_α is given by a generalized Langevin equation,

$$\frac{\partial n_\alpha}{\partial t} = -\gamma \frac{\delta F}{\delta n_\alpha} + \eta_\alpha, \quad (3)$$

where γ is a relaxation constant, and η_α is a Gaussian white noise term with $\langle \eta_\alpha(\mathbf{r}, t) \rangle_\eta = 0$ and

$$\langle \eta_\alpha(\mathbf{r}, t) \eta_\beta(\mathbf{r}', t') \rangle_\eta = 2\gamma T \delta_{\alpha\beta} \delta(\mathbf{r} - \mathbf{r}') \delta(t - t'). \quad (4)$$

$\langle \dots \rangle_\eta$ denotes an average over all realizations of the noise term η_α . The noise correlator in Eq. (4) is determined

by the requirement that in the absence of external perturbations the system relaxes into its equilibrium state as given by the Gibbs distribution. We show below that this is the case by comparing our results to those obtained within an equilibrium treatment of the same model.

The purpose of the following calculation is, ultimately, to calculate the response of currents to small perturbations. To this end we consider the generating functional²⁵

$$Z[J] = \left\langle \int \mathcal{D}n \det M \delta \left(\frac{\partial n_\alpha}{\partial t} + \gamma \frac{\delta F}{\delta n_\alpha} - \eta_\alpha \right) \times e^{\int d^2r dt \sum_\alpha J_\alpha n_\alpha} \right\rangle_\eta, \quad (5)$$

from which expectation values of various functions of n_α may be obtained by differentiation with respect to J . Here, $\det M$ is a Jacobian determinant, such that

$$\int \mathcal{D}n \det M \delta \left(\frac{\partial n_\alpha}{\partial t} + \gamma \frac{\delta F}{\delta n_\alpha} - \eta_\alpha \right) = 1, \quad (6)$$

where the matrix M itself is given by

$$M_{\alpha\beta}(\mathbf{r}, t; \mathbf{r}', t') = \frac{\delta}{\delta n_\beta(\mathbf{r}', t')} \left[\frac{\partial n_\alpha(\mathbf{r}, t)}{\partial t} + \gamma \frac{\delta F}{\delta n_\alpha(\mathbf{r}, t)} - \eta_\alpha(\mathbf{r}, t) \right]. \quad (7)$$

In Appendix A we evaluate the Jacobian determinant, and show that²⁵

$$\det M = \exp \left[\frac{\gamma u}{2} \left(1 + \frac{2}{N} \right) \delta(0) \int d^2r dt \sum_\alpha n_\alpha^2 \right]. \quad (8)$$

The path integral in Eq. (5), with the appropriate Jacobian, is constrained such that for each realization of η_α , only the configuration which solves the equations of motion, Eq. (3), is included. In order to manage the path integral over the delta functions, which enforce this constraint, we write them using auxiliary fields, \tilde{n}_α ,

$$Z[J] = \left\langle \int \mathcal{D}n \mathcal{D}\tilde{n} e^{\int d^2r dt \sum_\alpha \left\{ i\tilde{n}_\alpha \left(\frac{\partial n_\alpha}{\partial t} + \gamma \frac{\delta F}{\delta n_\alpha} - \eta_\alpha \right) + \frac{\gamma u}{2} \left(1 + \frac{2}{N} \right) \delta(0) n_\alpha^2 + J_\alpha n_\alpha \right\}} \right\rangle_\eta. \quad (9)$$

At this stage, it is simple to perform the average over all realization of the noise terms, η_α , yielding

$$Z[J] = \int \mathcal{D}n \mathcal{D}\tilde{n} e^{\int d^2r dt \sum_\alpha \left\{ i\tilde{n}_\alpha \left(\frac{\partial n_\alpha}{\partial t} + \gamma \frac{\delta F}{\delta n_\alpha} \right) - \gamma T \tilde{n}_\alpha^2 + \frac{\gamma u}{2} \left(1 + \frac{2}{N} \right) \delta(0) n_\alpha^2 + J_\alpha n_\alpha \right\}}. \quad (10)$$

By substituting the free energy derivative, and rotating $i\tilde{n}_\alpha \rightarrow \tilde{n}_\alpha$, we can finally write the generating functional

$$Z[J] = \int \mathcal{D}n \mathcal{D}\tilde{n} e^{-S[\tilde{n}, n] + \int d^2r dt \sum_\alpha J_\alpha n_\alpha}, \quad (11)$$

in terms of the action

$$S[\tilde{n}, n] = - \int d^2r dt \left\{ \frac{1}{2} \sum_{\alpha} (\tilde{n}_{\alpha} \ n_{\alpha}) \begin{pmatrix} 2\gamma T & L^+ \\ L^- & \gamma u (1 + \frac{2}{N}) \delta(0) \end{pmatrix} \begin{pmatrix} \tilde{n}_{\alpha} \\ n_{\alpha} \end{pmatrix} + \frac{\gamma u}{N} \sum_{\alpha\beta} \tilde{n}_{\alpha} n_{\alpha} n_{\beta} n_{\beta} \right\}, \quad (12)$$

where we have defined $L^{\pm} = \pm \partial/\partial t - \gamma \rho_s \nabla^2 - \gamma u$. The action, Eq. (12), contains a quartic term, and therefore cannot be easily used to evaluate response functions. Furthermore, we are interested in results for the NLSM, obtained by taking $u \rightarrow \infty$, which rules out the possibility of treating the quartic term perturbatively. Some progress can be made, though, using a saddle-point approximation, as is described in the next section.

III. SADDLE-POINT APPROXIMATION

The quartic interaction term in Eq. 12 can be decoupled by introducing two decoupling fields, $\bar{\sigma}$ and $\bar{\lambda}$,²⁸

$$e^{\int d^2r dt \frac{\gamma u}{N} \sum_{\alpha\beta} \tilde{n}_{\alpha} n_{\alpha} n_{\beta} n_{\beta}} = \int \mathcal{D}\bar{\sigma} \mathcal{D}\bar{\lambda} e^{\int d^2r dt \{ \bar{\sigma} \sum_{\alpha} \tilde{n}_{\alpha} n_{\alpha} + \bar{\lambda} \sum_{\beta} n_{\beta} n_{\beta} - \frac{N}{\gamma u} \bar{\sigma} \bar{\lambda} \}}. \quad (13)$$

The resulting action, which includes also these decoupling fields, is

$$S[\tilde{n}, n, \bar{\sigma}, \bar{\lambda}] = - \int d^2r dt \left\{ \frac{1}{2} \sum_{\alpha} (\tilde{n}_{\alpha} \ n_{\alpha}) \begin{pmatrix} 2\gamma T & L^+ + \bar{\sigma} \\ L^- + \bar{\sigma} & \gamma u (1 + \frac{2}{N}) \delta(0) + 2\bar{\lambda} \end{pmatrix} \begin{pmatrix} \tilde{n}_{\alpha} \\ n_{\alpha} \end{pmatrix} - \frac{N}{\gamma u} \bar{\sigma} \bar{\lambda} \right\}. \quad (14)$$

It is now possible to integrate over \tilde{n}_{α} and n_{α} , leaving us with an action that depends only on $\bar{\sigma}$ and $\bar{\lambda}$,

$$S[\bar{\sigma}, \bar{\lambda}] = \frac{N}{2} \text{Tr} \ln \begin{pmatrix} 2\gamma T & L^+ + \bar{\sigma} \\ L^- + \bar{\sigma} & \gamma u (1 + \frac{2}{N}) \delta(0) + 2\bar{\lambda} \end{pmatrix} + \frac{N}{\gamma u} \int d^2r dt \bar{\sigma} \bar{\lambda}. \quad (15)$$

In the limit $N \rightarrow \infty$ the decoupling fields obtain uniform values determined by the saddle-point equations

$$\frac{\delta S}{\delta \bar{\sigma}} = \frac{N}{2} \int \frac{d^2p d\omega}{(2\pi)^3} \frac{L^+(\mathbf{p}, \omega) + L^-(\mathbf{p}, \omega) + 2\bar{\sigma}}{2\gamma T[\gamma u \delta(0) + 2\bar{\lambda}] - [L^+(\mathbf{p}, \omega) + \bar{\sigma}][L^-(\mathbf{p}, \omega) + \bar{\sigma}]} - \frac{N\bar{\lambda}}{\gamma u} = 0 \quad (16)$$

$$\frac{\delta S}{\delta \bar{\lambda}} = \frac{N}{2} \int \frac{d^2p d\omega}{(2\pi)^3} \frac{4\gamma T}{2\gamma T[\gamma u \delta(0) + 2\bar{\lambda}] - [L^+(\mathbf{p}, \omega) + \bar{\sigma}][L^-(\mathbf{p}, \omega) + \bar{\sigma}]} + \frac{N\bar{\sigma}}{\gamma u} = 0, \quad (17)$$

where $L^{\pm}(\mathbf{p}, \omega) = \mp i\omega + \gamma \rho_s p^2 - \gamma u$. The first saddle-point equation is solved by²⁹

$$\bar{\lambda} = -\frac{1}{2} \gamma u \delta(0), \quad (18)$$

while the second takes the form

$$\frac{\bar{\sigma}}{\gamma u} = \int \frac{d^2p}{(2\pi)^2} \frac{\gamma T}{\gamma \rho_s p^2 + \bar{\sigma} - \gamma u}. \quad (19)$$

Defining an inverse correlation length, m , such that

$$\bar{\sigma} = \gamma \rho_s m^2 + \gamma u, \quad (20)$$

gives in the limit $u \rightarrow \infty$,

$$1 = \int \frac{d^2p}{(2\pi)^2} \frac{T/\rho_s}{p^2 + m^2}, \quad (21)$$

that is identical to the saddle-point equation derived within an equilibrium treatment of the NLSM²³. This

provides justification for our choice of the noise correlator, Eq. (4). Eq. (21) is solved to give

$$m^2 = \Lambda^2 \left[\exp\left(\frac{4\pi\rho_s}{T}\right) - 1 \right]^{-1}, \quad (22)$$

where Λ is an ultra-violet cutoff on the momenta. In the following we assume that $m < \Lambda$, implying $T \lesssim 4\pi\rho_s$. At higher temperatures one needs to put the model, Eq. (1), on a lattice.

At this point, it is convenient to shift the decoupling fields, such that their saddle-point values vanish in equilibrium, *i.e.*, $\bar{\sigma} = \sigma + \gamma \rho_s m^2 + \gamma u$ and $\bar{\lambda} = \lambda - \gamma u \delta(0)/2$. By defining

$$(g^{\pm})^{-1} = \pm \frac{\partial}{\partial t} + \gamma \rho_s (-\nabla^2 + m^2), \quad (23)$$

we can write the action in a form

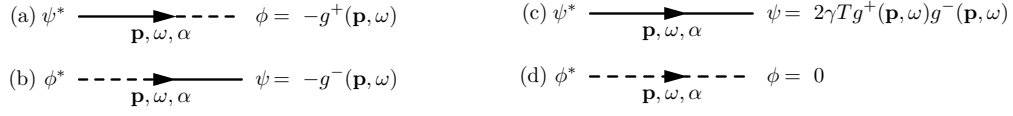


FIG. 1: Propagator diagrams.

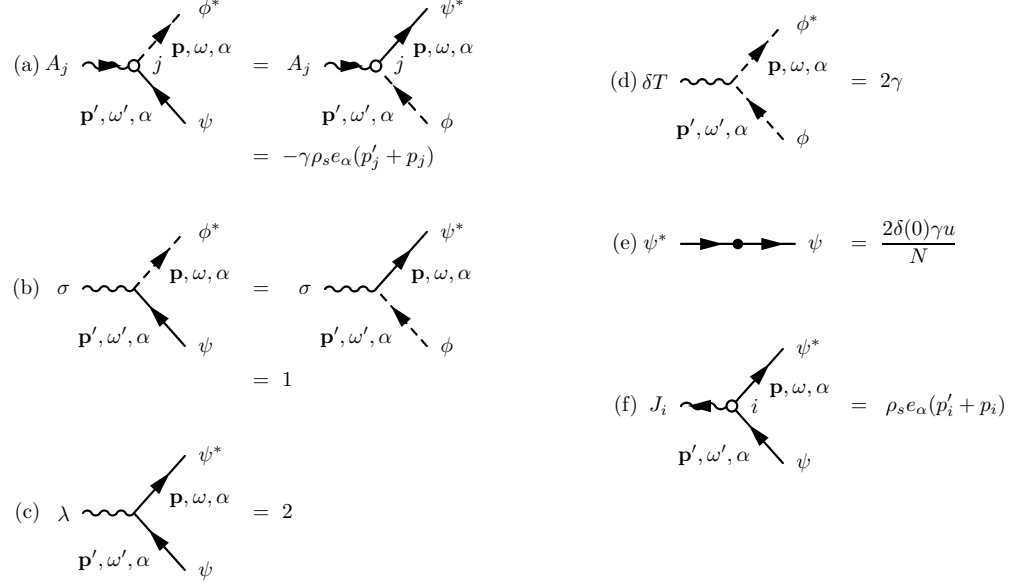


FIG. 2: Vertex diagrams.

$$S[\tilde{n}, n, \sigma, \lambda] = - \int d^2r dt \left\{ \frac{1}{2} \sum_{\alpha} (\tilde{n}_{\alpha} \ n_{\alpha}) \begin{pmatrix} 2\gamma T & (g^+)^{-1} + \sigma \\ (g^-)^{-1} + \sigma & 2\lambda + 2\gamma u \delta(0)/N \end{pmatrix} \begin{pmatrix} \tilde{n}_{\alpha} \\ n_{\alpha} \end{pmatrix} - \frac{N}{\gamma u} (\sigma + \gamma \rho_s m^2 + \gamma u) (\lambda - \gamma u \delta(0)/2) \right\}, \quad (24)$$

which is most appropriate for handling the limit $N \rightarrow \infty$. In this limit, and in the absence of perturbing forces, the functional integrals over σ and λ are dominated by their saddle point configurations $\sigma = \lambda = 0$. However, when the system is perturbed out of equilibrium, as we consider next, these values may change. In addition, fluctuations in σ and λ must be considered when extending the calculation to order $\mathcal{O}(1/N)$.

IV. DIAGRAMATIC PERTURBATION THEORY

In order to couple some of the fields to an electromagnetic potential \mathbf{A} , we construct the following complex fields from consecutive pairs of real fields

$$\psi_{\alpha} = \frac{1}{\sqrt{2}}(n_{2\alpha-1} + in_{2\alpha}) \quad \phi_{\alpha} = \frac{1}{\sqrt{2}}(\tilde{n}_{2\alpha-1} + i\tilde{n}_{2\alpha}). \quad (25)$$

After minimal coupling to \mathbf{A} , the free energy, Eq. (1), becomes

$$F = \int d^2r \left\{ \rho_s \sum_{\alpha=1}^{N/2} |(-i\nabla - e_{\alpha}\mathbf{A})\psi_{\alpha}|^2 + \frac{u}{4N} \left(2 \sum_{\alpha=1}^{N/2} |\psi_{\alpha}|^2 - N \right)^2 \right\}, \quad (26)$$

where e_{α} is the charge of field ψ_{α} , in units where $\hbar = c = 1$. Similarly, the coupling to \mathbf{A} and the presence of a weak time-dependent temperature gradient δT introduce additional terms to the action, Eq. (24). In preparation for

constructing a diagrammatic perturbation theory, we separate the action into two parts $S[\phi, \psi, \sigma, \lambda] = S_0[\phi, \psi, \sigma, \lambda] + S_1[\phi, \psi, \sigma, \lambda]$, where in the latter we keep only terms linear in \mathbf{A} , hence restricting the calculation to linear response

$$S_0 = - \int d^2r dt \sum_{\alpha=1}^{N/2} \left\{ (\phi_\alpha^* \ \psi_\alpha^*) \begin{pmatrix} 2\gamma T & (g^+)^{-1} \\ (g^-)^{-1} & 0 \end{pmatrix} \begin{pmatrix} \phi_\alpha \\ \psi_\alpha \end{pmatrix} - \frac{N}{\gamma u} (\sigma + \gamma \rho_s m^2 + \gamma u) (\lambda - \gamma u \delta(0)/2) \right\}, \quad (27)$$

$$S_1 = - \int d^2r dt \sum_{\alpha=1}^{N/2} (\phi_\alpha^* \ \psi_\alpha^*) \begin{pmatrix} 2\gamma \delta T & \gamma \rho_s e_\alpha \{\mathbf{A}, i \nabla\} + \sigma \\ \gamma \rho_s e_\alpha \{\mathbf{A}, i \nabla\} + \sigma & 2\lambda + 2\gamma u \delta(0)/N \end{pmatrix} \begin{pmatrix} \phi_\alpha \\ \psi_\alpha \end{pmatrix}. \quad (28)$$

Eq. (27) defines the ψ and ϕ propagators, whose diagrammatic representation is given in Fig. 1, with

$$g^\pm(\mathbf{p}, \omega) = \frac{1}{\mp i\omega + \gamma \rho_s (p^2 + m^2)}. \quad (29)$$

The various interaction terms in Eq. (28) are given by the vertices in Figs. 2a-e. To these we add a vertex, Figure 2f, for the paramagnetic current $\mathbf{J} = -\frac{\delta F}{\delta \mathbf{A}}|_{\mathbf{A}=0}$, with F given by Eq. (26),

$$\mathbf{J} = i\rho_s \sum_{\alpha=1}^{N/2} e_\alpha [(\nabla \psi_\alpha^*) \psi_\alpha - \psi_\alpha^* \nabla \psi_\alpha]. \quad (30)$$

Eq. (27) also contains source terms for the fields σ and λ , as shown in Fig. 3a-b. However, they are canceled by the diagrams in Fig. 3c-d, in what is a diagrammatic representation of the saddle-point equations, Eqs. (16,17), as can be verified once one notices that the sum over α runs up to $N/2$ after the model is written using complex fields. Finally, S_0 defines the bare propagators, G_0 , for σ and λ . The dressed propagators, to order $\mathcal{O}(1/N)$, can be constructed using a Dyson equation $G^{-1} = G_0^{-1} - \Sigma$,

$$\begin{pmatrix} G_{\sigma\sigma} & G_{\sigma\lambda} \\ G_{\lambda\sigma} & G_{\lambda\lambda} \end{pmatrix}^{-1} = \begin{pmatrix} 0 & \frac{\gamma u}{N} \\ \frac{\gamma u}{N} & 0 \end{pmatrix}^{-1} - N \begin{pmatrix} \Pi_{\sigma\sigma} & \Pi_{\sigma\lambda} \\ \Pi_{\lambda\sigma} & \Pi_{\lambda\lambda} \end{pmatrix}, \quad (31)$$

$$\begin{aligned} \text{(a)} \quad \sigma \text{ wavy line} &= \frac{1}{2} N \delta(0) \\ \text{(b)} \quad \lambda \text{ wavy line} &= -N \left(\frac{\rho_s m^2}{u} + 1 \right) \\ \text{(c)} \quad \sigma \text{ wavy line} + \sigma \text{ wavy line} \begin{array}{c} \circlearrowleft \\ \text{p, } \omega, \alpha \end{array} & \\ &+ \sigma \text{ wavy line} \begin{array}{c} \circlearrowright \\ \text{p, } \omega, \alpha \end{array} = 0 \\ \text{(d)} \quad \lambda \text{ wavy line} + \lambda \text{ wavy line} \begin{array}{c} \circlearrowleft \\ \text{p, } \omega, \alpha \end{array} & \\ &+ \lambda \text{ wavy line} \begin{array}{c} \circlearrowright \\ \text{p, } \omega, \alpha \end{array} = 0 \end{aligned}$$

FIG. 3: Diagrammatic representation of the saddle-point equations, Eqs. (16) and (17)

$$\begin{aligned} \text{(a)} \quad N\Pi_{\sigma\sigma}(\mathbf{Q}, \Omega) &= \\ & \begin{array}{c} \text{p} + \mathbf{Q}, \omega + \Omega, \alpha \\ \sigma \text{ wavy line} \begin{array}{c} \circlearrowleft \\ \text{p, } \omega, \alpha \end{array} + \sigma \text{ wavy line} \begin{array}{c} \circlearrowright \\ \text{p, } \omega, \alpha \end{array} \end{array} = 0 \\ \text{(b)} \quad N\Pi_{\sigma\lambda}(\mathbf{Q}, \Omega) &= \\ & \begin{array}{c} \text{p} + \mathbf{Q}, \omega + \Omega, \alpha \\ \sigma \text{ wavy line} \begin{array}{c} \circlearrowleft \\ \text{p, } \omega, \alpha \end{array} \lambda \text{ wavy line} + \sigma \text{ wavy line} \begin{array}{c} \circlearrowright \\ \text{p, } \omega, \alpha \end{array} \lambda \text{ wavy line} \end{array} \\ \text{(c)} \quad N\Pi_{\lambda\lambda}(\mathbf{Q}, \Omega) &= \\ & \begin{array}{c} \text{p} + \mathbf{Q}, \omega + \Omega, \alpha \\ \lambda \text{ wavy line} \begin{array}{c} \circlearrowleft \\ \text{p, } \omega, \alpha \end{array} \lambda \text{ wavy line} \end{array} \end{aligned}$$

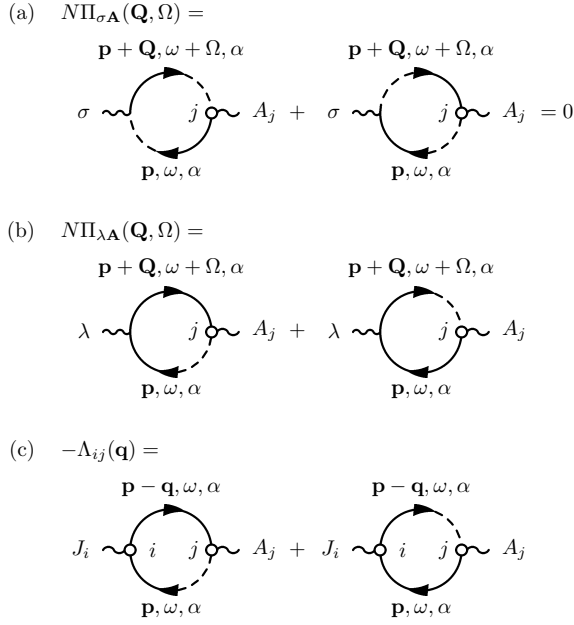
FIG. 4: Polarization diagrams for the σ and λ fields.

where the polarization diagrams, $\Pi(\mathbf{Q}, \Omega)$, are given in Figure 4. Since the poles of the bubbles in Fig. 4a reside on the same half of the complex (\mathbf{p}, ω) plane we find that $\Pi_{\sigma\sigma} = 0$. This leads in the limit $u \rightarrow \infty$ to

$$\begin{aligned} \begin{pmatrix} G_{\sigma\sigma} & G_{\sigma\lambda} \\ G_{\lambda\sigma} & G_{\lambda\lambda} \end{pmatrix} &= -\frac{1}{N} \begin{pmatrix} 0 & \Pi_{\sigma\lambda} \\ \Pi_{\lambda\sigma} & \Pi_{\lambda\lambda} \end{pmatrix}^{-1} \\ &= -\frac{1}{N} \begin{pmatrix} -\frac{\Pi_{\lambda\lambda}}{(\Pi_{\sigma\lambda})^2} & \frac{1}{\Pi_{\sigma\lambda}} \\ \frac{1}{\Pi_{\lambda\sigma}} & 0 \end{pmatrix}. \quad (32) \end{aligned}$$

V. DIAMAGNETIC SUSCEPTIBILITY

Before calculating the electric current's response to a static weak magnetic field, we first show that in the presence of such a perturbation σ and λ remain unchanged. To this end we need to calculate the diagrams in Fig. 5a-b, which contain the leading order contribution to the response of σ and λ to A_j . An examination of the pole structure of Fig. 5a leads to $\Pi_{\sigma\mathbf{A}}(\mathbf{Q}, \Omega = 0) = 0$. In Ap-

FIG. 5: Response of σ , λ and J_i to A_j

pendix B we explicitly calculate the diagrams appearing in Fig. 5b and find that also $\Pi_{\lambda\mathbf{A}}(\mathbf{Q}, \Omega = 0) = 0$.

To calculate the magnetization we note that the equilibrium magnetization currents are given by $\mathbf{J} = \nabla \times \mathbf{M}$ (this is a consequence of $\nabla \cdot \mathbf{J} = 0$ for the magnetization currents and is taken as the definition of \mathbf{M}). Therefore, in the xy plane, $J_i = \varepsilon_{ij} \partial_j M_z$, where ε_{ij} is the antisymmetric tensor with $\varepsilon_{xy} = -\varepsilon_{yx} = 1$. The susceptibility χ is the ratio between M_z and $B_z = \varepsilon_{ij} \partial_i A_j$. As a result,

$$J_i(\mathbf{q}) = \chi(\delta_{ij} q^2 - q_i q_j) A_j(\mathbf{q}), \quad (33)$$

from which it follows that χ itself can be calculated by identifying a term proportional to $q_i q_j$ in the response function $\Lambda_{ij}(\mathbf{q})$, defined via $J_i(\mathbf{q}) = -\Lambda_{ij}(\mathbf{q}) A_j(\mathbf{q})$. The diagrammatic representation of the latter is given in Fig. 5c and evaluated in Appendix B. The result is

$$-\Lambda_{ij}(\mathbf{q}) = \frac{\overline{e^2} T}{2\pi} \left[\log \left(\frac{\Lambda^2}{m^2} \right) - 1 \right] \delta_{ij} - \frac{\overline{e^2} T}{12\pi m^2} (\delta_{ij} q^2 - q_i q_j), \quad (34)$$

where

$$\overline{e^2} \equiv \sum_{\alpha=1}^{N/2} e_{\alpha}^2. \quad (35)$$

The $q = 0$ piece in Eq. (34) should get canceled by the diamagnetic contribution to the current, which is given

by $-2\overline{e^2} \rho_s \langle \psi_{\alpha}^* \psi_{\alpha} \rangle \mathbf{A}$. Its contribution to $-\Lambda_{ij}$ is

$$\begin{aligned} -2\overline{e^2} \rho_s \delta_{ij} \int_{\mathbf{p}\omega} 2\gamma T g^+ g^-(\mathbf{p}, \omega) &= -2\overline{e^2} T \delta_{ij} \int_{\mathbf{p}} \frac{1}{p^2 + m^2} \\ &= -\frac{\overline{e^2} T}{2\pi} \log \left(\frac{\Lambda^2}{m^2} \right) \delta_{ij}. \end{aligned} \quad (36)$$

The imperfect cancelation is due to the non gauge-invariant cutoff scheme which we used²³. From Eq. (34) we nevertheless obtain

$$\chi = -\frac{\overline{e^2} T}{12\pi m^2}, \quad (37)$$

which is identical to the result calculated using equilibrium methods in Ref. 23. In terms of the inverse correlation length, m , this is also what one finds using the Gaussian approximation of the Ginzburg-Landau model.

VI. THE COEFFICIENT α_{xy}

The transverse thermoelectric transport coefficient, α_{xy} , is defined via $J_x = \alpha_{xy}(-\partial_y T)$, which we rewrite as

$$J_i = \frac{\alpha_{xy}}{B} \varepsilon_{lj} \partial_l A_j \varepsilon_{ik} (-\partial_k T). \quad (38)$$

This Fourier transforms into

$$J_i(\mathbf{q} + \mathbf{Q}) = \frac{\alpha_{xy}}{B} (-\delta_{ij} \mathbf{q} \cdot \mathbf{Q} + Q_i q_j) T(\mathbf{q}) A_j(\mathbf{Q}), \quad (39)$$

from which we conclude that the coefficient α_{xy}/B can be obtained by calculating the response of J_i to δT and A_j , and reading off the term proportional to $Q_i q_j$.

In order to calculate this response, we first examine the change in the saddle-point values of σ and λ in the presence of a slow temperature gradient. The change in σ is given by Fig. 6a,

$$\frac{\sigma(\mathbf{Q}, \Omega)}{\delta T(\mathbf{Q}, \Omega)} = -\frac{2\gamma}{\Pi_{\sigma\lambda}(\mathbf{Q}, \Omega)} \int_{\mathbf{p}\omega} g^-(\mathbf{p}, \omega) g^+(\mathbf{p} + \mathbf{Q}, \omega + \Omega), \quad (40)$$

where we have used $G_{\sigma\lambda}(\mathbf{Q}, \Omega) = -1/N\Pi_{\sigma\lambda}(\mathbf{Q}, \Omega)$, see Eq. (32). On the other hand, the temperature derivative of the saddle-point equation (21) can be represented as

$$\begin{aligned} 0 &= \frac{d}{dT} \int_{\mathbf{p}\omega} 2\gamma T g^+(\mathbf{p}, \omega) g^-(\mathbf{p}, \omega) \\ &= \int_{\mathbf{p}\omega} 2\gamma g^+(\mathbf{p}, \omega) g^-(\mathbf{p}, \omega) \\ &\quad + 2\gamma T \frac{dm^2}{dT} \frac{d}{dm^2} \int_{\mathbf{p}\omega} g^+(\mathbf{p}, \omega) g^-(\mathbf{p}, \omega) \\ &= \int_{\mathbf{p}\omega} g^+(\mathbf{p}, \omega) g^-(\mathbf{p}, \omega) + \frac{\rho_s}{2} \frac{dm^2}{dT} \Pi_{\sigma\lambda}(\mathbf{Q} = 0, \Omega = 0), \end{aligned} \quad (41)$$

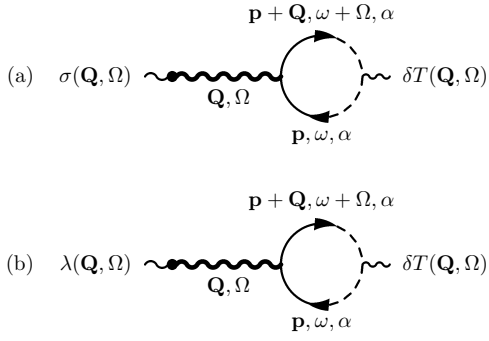


FIG. 6: Response of σ and λ to δT . The bold wavy line represents, G , the dressed propagator of σ and λ , given by Eq. (32).

where we have used the relation

$$\Pi_{\sigma\lambda}(\mathbf{Q} = 0, \Omega = 0) = \frac{2T}{\rho_s} \frac{d}{dm^2} \int_{\mathbf{p}\omega} g^+(\mathbf{p}, \omega) g^-(\mathbf{p}, \omega), \quad (42)$$

which is readily verified from the algebraic expression of the diagrams for $\Pi_{\sigma\lambda}$, Fig. 4b. Combining Eqs. (40) and (41) establishes that *in the limit* $\mathbf{Q}, \Omega \rightarrow 0$

$$\sigma = \gamma \rho_s \frac{dm^2}{dT} \delta T. \quad (43)$$

Finally, one finds, with the help of Fig. 6b and $G_{\lambda\lambda} = 0$, that the equilibrium result $\lambda = 0$ is unaffected by the temperature gradient.

As a consequence of the above discussion, α_{xy} acquires contributions both from the direct response to a gradient in δT and from the induced change in σ . The diagrams in Fig. 7a give the response to $\nabla \delta T$, while assuming that σ remains at its equilibrium value $\sigma = 0$. They are calculated in Appendix B up to leading order in $Q_i q_j$, with the result

$$\Delta_{\delta T} \approx \delta_{ij}(\dots) + q_i Q_j(\dots) + Q_i q_j \frac{\overline{e^2}}{8\pi m^2}. \quad (44)$$

To this we need to add the response to $\nabla \sigma$, as represented by the diagrams in Fig. 7b. They are also calculated in Appendix B, and up to leading order in $Q_i q_j$ give

$$\Delta_{\sigma} \approx \delta_{ij}(\dots) + q_i Q_j(\dots) - Q_i q_j \frac{\overline{e^2} T}{12\pi \gamma \rho_s m^4}. \quad (45)$$

Part of the response to a temperature gradient in the bulk, $\delta J_i = \epsilon_{ij} B \frac{d\chi}{dT} \partial_j \delta T$, is due to redistribution of equilibrium magnetization currents, and should be subtracted from the calculated bulk current, since it is canceled by opposite currents on the system edges³⁰. This amounts to adding $\partial\chi/\partial T$ to the above calculated α_{xy}/B , with the resulting transport response,

$$\begin{aligned} \frac{\alpha_{xy}^{\text{tr}}}{B} &= \frac{\partial \Delta_{\delta T}}{\partial(Q_x q_y)} + \frac{\partial \Delta_{\sigma}}{\partial(Q_x q_y)} \frac{d\sigma}{d\delta T} + \frac{\partial \chi}{\partial T} \\ &= \frac{\overline{e^2}}{24\pi m^2} = -\frac{\chi}{2T}. \end{aligned} \quad (46)$$

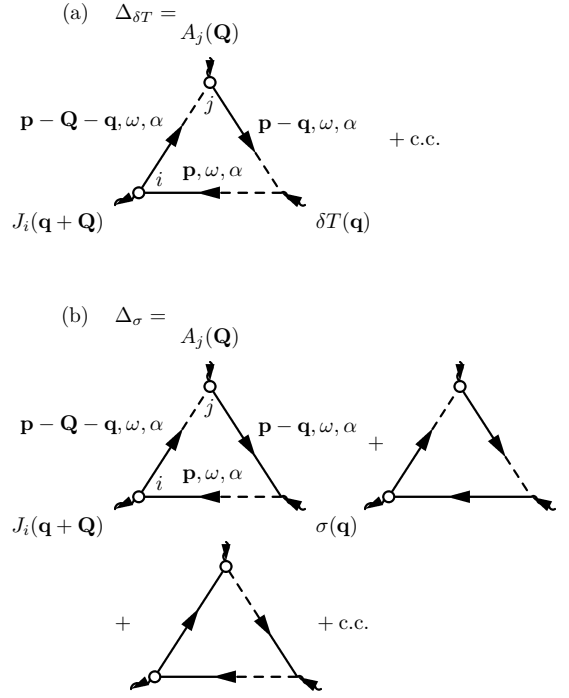


FIG. 7: Thermoelectric response diagrams.

This is our main result, which in terms of the inverse correlation length, m , agrees with Ussishkin *et al.*'s result for the Gaussian TDGL model⁸.

VII. DISCUSSION

While we derived our main result, Eq. (46), for the fully $O(N)$ symmetric NLSM, one expects the Hamiltonian of generic systems, including the underdoped cuprates, to contain terms which explicitly break the symmetry. It is a simple task to adapt our calculation to a case where the symmetry breaking terms are quadratic in the fields. For example, the model may include different values of the stiffness for different fields, or additional mass terms. In such a case one only needs to incorporate these changes into the propagators, via Eq. (29). The final result is the same, when written in terms of the inverse correlation length m , which itself is still a solution of a saddle-point equation, similar to Eq. (21), but adapted to the non-symmetric model. If, on the other hand, the symmetry breaking terms are of higher order, such as quartic terms which impose a square lattice point group symmetry on the CDW components²³, then additional decoupling fields are needed, and the adaptation is not as straightforward. Nevertheless, it is still reasonable to expect that the Nernst coefficient's dependence on the inverse correlation length m remains unchanged.

The saddle point approximation, which we use to arrive at Eq. (46), is strictly correct only in the $N \rightarrow \infty$ limit. However, it is still expected to describe the model's

behavior at high enough temperatures, since corrections of order $1/N$ become less important as the temperature is increased³¹. On the other hand, the approximation is likely to fail at low temperatures. This is especially true in the physically relevant case where the symmetry is broken so as to favor SC order. At low temperatures the symmetry reduces to $O(2)$, and the Nernst signal should be calculated within a SC vortex based model¹³. Thus, as the temperatures is increased, the Nernst effect is expected to crossover²² from vortex physics at low temperatures, to the Gaussian fluctuations result, which we calculated here, at high temperatures.

Acknowledgments

This research was supported by the Israel Science Foundation (Grant No. 585/13).

Appendix A: Evaluation of the Jacobian determinant

Evaluating the Jacobian determinant in the path integral, Eq. (5), can be made simple by separating the matrix $M_{\alpha\beta}(\mathbf{r}, t; \mathbf{r}', t')$, Eq. (7), into two parts. Defining

$$P_{\alpha\beta}(\mathbf{r}, t; \mathbf{r}', t') \equiv \frac{\partial}{\partial t} \delta_{\alpha\beta} \delta(\mathbf{r} - \mathbf{r}') \delta(t - t') \quad (\text{A1})$$

and

$$Q_{\alpha\beta}(\mathbf{r}, t; \mathbf{r}', t') \equiv \gamma \frac{\delta^2 F}{\delta n_\alpha(\mathbf{r}, t) \delta n_\beta(\mathbf{r}', t')}, \quad (\text{A2})$$

we have

$$\det M = \det P \det(1 + P^{-1}Q) = \det P e^{\text{Tr} \ln(1 + P^{-1}Q)}, \quad (\text{A3})$$

where

$$P_{\alpha\beta}^{-1}(\mathbf{r}, t; \mathbf{r}', t') = \theta(t - t') \delta_{\alpha\beta} \delta(\mathbf{r} - \mathbf{r}'). \quad (\text{A4})$$

$\det P$ is independent of the fields and, as such, can be disregarded. To evaluate the Jacobian we need only to expand the logarithm in Eq. (A3) in powers of $P^{-1}Q$. We find that aside from an irrelevant constant the linear term is given by

$$\text{Tr} P^{-1}Q = \gamma u \left(1 + \frac{2}{N}\right) \theta(0) \delta(0) \int d^2 r dt \sum_\alpha n_\alpha^2, \quad (\text{A5})$$

while the quadratic and higher terms vanish²⁵. A proper limiting process gives

$$\theta(0) = \frac{1}{2} \quad \text{and} \quad \delta(0) = \int \frac{d^2 p}{(2\pi)^2}. \quad (\text{A6})$$

where the integral is over the first Brillouin zone. This establishes Eq. (8), up to an unimportant normalization constant.

Appendix B: Evaluation of diagrams

In this appendix we calculate in detail those diagrams which are used in the main text. We begin by showing that λ remains zero in the presence of a static, weak magnetic field. To do so we evaluate the diagram in Fig. 5b for $\Omega = 0$,

$$N\Pi_{\lambda\mathbf{A}}(\mathbf{Q}, \Omega = 0) = 4 \sum_{\alpha=1}^{N/2} e_\alpha \gamma^2 \rho_s T \int_{\mathbf{p}\omega} (2p_j + Q_j) [g^-(\mathbf{p}, \omega) g^+ g^-(\mathbf{p} + \mathbf{Q}, \omega) + g^+ g^-(\mathbf{p}, \omega) g^+(\mathbf{p} + \mathbf{Q}, \omega)], \quad (\text{B1})$$

where here and throughout $\int_{\mathbf{p}\omega} \equiv \int \frac{d^2 p}{(2\pi)^2} \int \frac{d\omega}{2\pi}$ etc. The integrand has only simple poles, so integrating over ω gives

$$\begin{aligned} N\Pi_{\lambda\mathbf{A}}(\mathbf{Q}, \Omega = 0) &= \frac{2T}{\rho_s} \sum_\alpha e_\alpha \int_{\mathbf{p}} \frac{2p_j + Q_j}{(p^2 + m^2) [(p + \mathbf{Q})^2 + m^2]} \\ &= \frac{2T}{\rho_s} \sum_\alpha e_\alpha \int_{\mathbf{p}} \int_0^1 du \frac{2p_j + Q_j}{\{u(p^2 + m^2) + (1-u)[(p + \mathbf{Q})^2 + m^2]\}^2} \\ &= \frac{2T}{\rho_s} \sum_\alpha e_\alpha \int_0^1 du \int_{\mathbf{p}'} \frac{2p'_j - (1-2u)Q_j}{[p'^2 + m^2 + u(1-u)Q^2]^2} = 0, \end{aligned} \quad (\text{B2})$$

where we have transformed to $\mathbf{p}' = \mathbf{p} + (1-u)\mathbf{Q}$.

Eq. (33) implies that the response function Λ_{ij} can be used to calculate the diamagnetic susceptibility χ . The

diagrams for $\Lambda_{ij}(\mathbf{q})$ are given in Fig. 5c, and evaluate to

$$\begin{aligned}
-\Lambda_{ij}(\mathbf{q}) &= 2\bar{e}^2(\gamma\rho_s)^2T \int_{\mathbf{p}\omega} (2p_i - q_i)(2p_j - q_j) [g^-(\mathbf{p}, \omega)g^+g^-(\mathbf{p} - \mathbf{q}, \omega) + g^+g^-(\mathbf{p}, \omega)g^+(\mathbf{p} - \mathbf{q}, \omega)] \\
&= \bar{e}^2T \int_{\mathbf{p}} \frac{(2p_i - q_i)(2p_j - q_j)}{(p^2 + m^2)[(\mathbf{p} - \mathbf{q})^2 + m^2]} \\
&= \bar{e}^2T \int_{\mathbf{p}} \int_0^1 du \frac{(2p_i - q_i)(2p_j - q_j)}{\{u(p^2 + m^2) + (1 - u)[(\mathbf{p} - \mathbf{q})^2 + m^2]\}^2}, \tag{B3}
\end{aligned}$$

with $\bar{e}^2 = \sum_{\alpha=1}^{N/2} e_{\alpha}^2$. Next, we transform to $\mathbf{p}' = \mathbf{p} - (1 - u)\mathbf{q}$ and expand the integral in small \mathbf{q} , since we are interested in identifying its $\mathcal{O}(q^2)$ piece. As a result we find

$$\begin{aligned}
-\Lambda_{ij}(\mathbf{q} \rightarrow 0) &= 2\bar{e}^2T\delta_{ij} \int_0^1 du \int_{\mathbf{p}'} \left[\frac{p'^2}{(p'^2 + m^2)^2} - \frac{2u(1 - u)q^2 p'^2}{(p'^2 + m^2)^3} \right] + \bar{e}^2Tq_iq_j \int_0^1 du \int_{\mathbf{p}'} \frac{(1 - 2u)^2}{(p'^2 + m^2)^2} \\
&= \frac{\bar{e}^2T}{2\pi} \left[\log\left(\frac{\Lambda^2}{m^2}\right) - 1 \right] \delta_{ij} - \frac{\bar{e}^2T}{12\pi m^2} (\delta_{ij}q^2 - q_iq_j), \tag{B4}
\end{aligned}$$

where Λ is an ultra-violet cutoff on $|\mathbf{p}|$.

To calculate the transverse thermoelectric transport coefficient in weak magnetic fields, we need to consider diagrams with three legs. The direct response to a temperature gradient is diagrammatically given in Fig. 7a. Focusing only the leading terms in Q_iq_j , we find,

$$\begin{aligned}
\Delta_{\delta T} &= \sum_{\alpha} \int_{\mathbf{p}\omega} 2\gamma g^-(\mathbf{p}, \omega) e_{\alpha}\rho_s(2p_i - Q_i - q_i) g^+(\mathbf{p} - \mathbf{Q} - \mathbf{q}, \omega) \gamma e_{\alpha}\rho_s(2p_j - Q_j - 2q_j) g^+(\mathbf{p} - \mathbf{q}, \omega) \\
&\quad + \sum_{\alpha} \int_{\mathbf{p}\omega} 2\gamma g^-(\mathbf{p} + \mathbf{q}, \omega) \gamma e_{\alpha}\rho_s(2p_j + Q_j + 2q_j) g^-(\mathbf{p} + \mathbf{Q} + \mathbf{q}, \omega) e_{\alpha}\rho_s(2p_i + Q_i + q_i) g^+(\mathbf{p}, \omega) \\
&= 4\bar{e}^2 \int_{\mathbf{p}} \frac{(2p_i - Q_i - q_i)(2p_j - Q_j - 2q_j)}{[p^2 + (\mathbf{p} - \mathbf{Q} - \mathbf{q})^2 + 2m^2][p^2 + (\mathbf{p} - \mathbf{q})^2 + 2m^2]} \\
&= 4\bar{e}^2 \int_0^1 du \int_{\mathbf{p}} \frac{(2p_i - Q_i - q_i)(2p_j - Q_j - 2q_j)}{\{u[2p^2 + 2m^2 - 2\mathbf{p} \cdot (\mathbf{Q} + \mathbf{q}) + (\mathbf{Q} + \mathbf{q})^2] + (1 - u)[2p^2 + 2m^2 - 2\mathbf{p} \cdot \mathbf{q} + q^2]\}^2} \\
&= \bar{e}^2 \int_0^1 du \int_{\mathbf{p}} \frac{(2p_i - Q_i - q_i)(2p_j - Q_j - 2q_j)}{[p^2 + m^2 - \mathbf{p} \cdot (u\mathbf{Q} + \mathbf{q}) + \mathcal{O}(q^2, Q^2, \mathbf{q} \cdot \mathbf{Q})]^2} \\
&\approx \delta_{ij}(\dots) + q_iq_j(\dots) + \bar{e}^2Q_iq_j \int_0^1 du \int_{\mathbf{p}'} \frac{1 - u}{(p'^2 + m^2)^2} \\
&\approx \delta_{ij}(\dots) + q_iq_j(\dots) + Q_iq_j \frac{\bar{e}^2}{8\pi m^2}, \tag{B5}
\end{aligned}$$

where $\mathbf{p}' = \mathbf{p} - (u\mathbf{Q} + \mathbf{q})/2$. Similarly, we need to calculate the response to a gradient in σ , given by the diagrams in

Fig. 7b. Retaining again only the leading terms in $Q_i q_j$, we have,

$$\begin{aligned}
\Delta_\sigma &= - \sum_\alpha \int_{\mathbf{p}\omega} g^-(\mathbf{p}, \omega) e_\alpha \rho_s (2p_i - Q_i - q_i) g^+(\mathbf{p} - \mathbf{Q} - \mathbf{q}, \omega) \gamma e_\alpha \rho_s (2p_j - Q_j - 2q_j) 2\gamma T g^+ g^-(\mathbf{p} - \mathbf{q}, \omega) \\
&\quad - \sum_\alpha \int_{\mathbf{p}\omega} 2\gamma T g^+ g^-(\mathbf{p}, \omega) e_\alpha \rho_s (2p_i - Q_i - q_i) g^+(\mathbf{p} - \mathbf{Q} - \mathbf{q}, \omega) \gamma e_\alpha \rho_s (2p_j - Q_j - 2q_j) g^+(\mathbf{p} - \mathbf{q}, \omega) \\
&\quad - \sum_\alpha \int_{\mathbf{p}\omega} g^-(\mathbf{p}, \omega) e_\alpha \rho_s (2p_i - Q_i - q_i) 2\gamma T g^+ g^-(\mathbf{p} - \mathbf{Q} - \mathbf{q}, \omega) \gamma e_\alpha \rho_s (2p_j - Q_j - 2q_j) g^-(\mathbf{p} - \mathbf{q}, \omega) + \text{c.c.} \\
&= - \frac{2\bar{e}^2 T}{\gamma \rho_s} \int_{\mathbf{p}} \frac{(2p_i - Q_i - q_i)(2p_j - Q_j - 2q_j)}{(p^2 + m^2)[(\mathbf{p} - \mathbf{Q} - \mathbf{q})^2 + m^2][(\mathbf{p} - \mathbf{q})^2 + m^2]} \\
&= - \frac{4\bar{e}^2 T}{\gamma \rho_s} \int_0^1 du \int_0^{1-u} dv \int_{\mathbf{p}} \frac{(2p_i - Q_i - q_i)(2p_j - Q_j - 2q_j)}{\{p^2 + m^2 + u[(\mathbf{p} - \mathbf{Q} - \mathbf{q})^2 - p^2] + v[(\mathbf{p} - \mathbf{q})^2 - p^2]\}^3} \\
&= - \frac{4\bar{e}^2 T}{\gamma \rho_s} \int_0^1 du \int_0^{1-u} dv \int_{\mathbf{p}} \frac{(2p_i - Q_i - q_i)(2p_j - Q_j - 2q_j)}{\{\mathbf{p} - u\mathbf{Q} - (u+v)\mathbf{q}\}^2 + m^2 + \mathcal{O}(q^2, Q^2, \mathbf{q} \cdot \mathbf{Q})\}^3} \\
&\approx \delta_{ij}(\dots) + q_i Q_j(\dots) - Q_i q_j \frac{8\bar{e}^2 T}{\gamma \rho_s} \int_0^1 du \int_0^{1-u} dv \int_{\mathbf{p}'} \frac{(2u-1)(u+v-1)}{(p'^2 + m^2)^3} \\
&\approx \delta_{ij}(\dots) + q_i Q_j(\dots) - Q_i q_j \frac{\bar{e}^2 T}{12\pi\gamma\rho_s m^4}. \tag{B6}
\end{aligned}$$

-
- ¹ P. A. Lee, N. Nagaosa, and X. Wen, *Rev. Mod. Phys.* **78**, 17 (2006).
- ² V. J. Emery and S. A. Kivelson, *Nature (London)* **374**, 434 (1995).
- ³ For a review of earlier results see, R. P. Huebener, *Supercond. Sci. Technol.* **8**, 189 (1995).
- ⁴ Z. A. Xu, N.P. Ong, Y. Wang, T. Kakeshita, and S. Uchida, *Nature (London)* **406**, 486 (2000).
- ⁵ Y. Wang, Z. A. Xu, T. Kakeshita, S. Uchida, S. Ono, Y. Ando, and N. P. Ong, *Phys. Rev. B* **64**, 224519 (2001).
- ⁶ Y. Wang, L. Li, and N. P. Ong, *Phys. Rev. B* **73**, 024510 (2006).
- ⁷ R. P. Huebener and A. Seher, *Phys. Rev.* **181**, 701 (1969).
- ⁸ I. Ussishkin, S. L. Sondhi and D. A. Huse, *Phys. Rev. Lett.* **89** 287001 (2002).
- ⁹ A. Pourret, H. Aubin, J. Lesueur, C. A. Marrache-Kikuchi, L. Bergé, L. Dumoulin, and K. Behnia, *Nat. Phys.* **2**, 683 (2006).
- ¹⁰ K. Michaeli and A. M. Finkel'stein, *Phys. Rev. B* **80**, 214516 (2009).
- ¹¹ D. Podolsky, S. Raghu, and A. Vishwanath, *Phys. Rev. Lett.* **99** 117004 (2007).
- ¹² S. Raghu, D. Podolsky, A. Vishwanath, and D. A. Huse, *Phys. Rev. B* **78**, 184520 (2008).
- ¹³ G. Wachtel and D. Orgad, arXiv:1310.2993 (2013).
- ¹⁴ G. Ghiringhelli, M. Le Tacon, M. Minola, S. Blanco-Canosa, C. Mazzoli, N. B. Brookes, G. M. De Luca, A. Frano, D. G. Hawthorn, F. He, T. Loew, M. Moretti Sala, D. C. Peets, M. Salluzzo, E. Schierle, R. Sutarto, G. A. Sawatzky, E. Weschke, B. Keimer, and L. Braicovich, *Science* **337**, 821 (2012).
- ¹⁵ J. Chang, E. Blackburn, A. T. Holmes, N. B. Christensen, J. Larsen, J. Mesot, R. Liang, D. A. Bonn, W. N. Hardy, A. Watenphul, M. v. Zimmermann, E. M. Forgan, and S. M. Hayden, *Nature Phys.* **8**, 871 (2012).
- ¹⁶ A. J. Achkar, R. Sutarto, X. Mao, F. He, A. Frano, S. Blanco-Canosa, M. Le Tacon, G. Ghiringhelli, L. Braicovich, M. Minola, M. Moretti Sala, C. Mazzoli, R. Liang, D. A. Bonn, W. N. Hardy, B. Keimer, G. A. Sawatzky, and D. G. Hawthorn, *Phys. Rev. Lett.* **109**, 167001 (2012).
- ¹⁷ A. J. Achkar, X. Mao, C. McMahan, R. Sutarto, F. He, R. Liang, D. A. Bonn, W. N. Hardy, and D. G. Hawthorn, *Phys. Rev. Lett.* **113**, 107002 (2014).
- ¹⁸ R. Comin, A. Frano, M. M. Yee, Y. Yoshida, H. Eisaki, E. Schierle, E. Weschke, R. Sutarto, F. He, A. Soumyanarayanan, Yang He, M. Le Tacon, I. S. Elfimov, J. E. Hoffman, G. A. Sawatzky, B. Keimer, and A. Damascelli, *Science* **343**, 390 (2014).
- ¹⁹ R. Comin, R. Sutarto, F. He, E. da Silva Neto, L. Chauviere, A. Frano, R. Liang, W. N. Hardy, D. Bonn, Y. Yoshida, H. Eisaki, J. E. Hoffman, B. Keimer, G. A. Sawatzky, and A. Damascelli, arXiv:1402.5415 (2014).
- ²⁰ E. H. da Silva Neto, P. Aynajian, A. Frano, R. Comin, E. Schierle, E. Weschke, A. Gyenis, J. Wen, J. Schneeloch, Z. Xu, S. Ono, G. Gu, M. Le Tacon, and A. Yazdani, *Science* **343**, 393 (2014).
- ²¹ A. Hackl, M. Vojta, and S. Sachdev, *Phys. Rev. B* **81**, 045102 (2010).
- ²² G. Wachtel and D. Orgad, unpublished.
- ²³ L. E. Hayward, D. G. Hawthorn, R. G. Melko, and

- S. Sachdev, *Science* **343**, 1336 (2014).
- ²⁴ P. C. Hohenberg and B. I. Halperin, *Rev. Mod. Phys.* **49**, 435 (1977).
- ²⁵ C. De Dominicis and L. Peliti, *Phys. Rev. B* **18**, 353 (1978).
- ²⁶ P. C. Martin, E. D. Siggia, and H. A. Rose, *Phys. Rev. A* **8**, 423 (1973).
- ²⁷ D. Podolsky and S. Sachdev, *Phys. Rev. B* **86**, 054508 (2012).
- ²⁸ This transformation is mathematically well defined provided the integration contour at infinity is along the line $\text{Im}(\lambda + \sigma) = \text{Re}(\lambda - \sigma) = 0$.
- ²⁹ For the model to obey the fluctuation-dissipation theorem in the limit $N \rightarrow \infty$, it is required that the n_α^2 terms in the action vanish. The given solution ensures this to the desired accuracy.
- ³⁰ N. R. Cooper, B. I. Halperin, and I. M. Ruzin, *Phys. Rev. B* **55**, 2344 (1997).
- ³¹ It is a rather difficult task to calculate the $1/N$ corrections themselves, due to the non-trivial analytical form of the polarization diagrams in Figs. 4b,c as a function of frequency Ω .